

# Study the Stochastic Perception of Refractive Index Variability of Ionosphere

Syed Nazeer Alam and Muhammad Ayub Khan Yousufzai

**Abstract**— It is said that ionosphere plays a vital role on electromagnetic waves (3 to 30 MHz) transmitted from ground station and after striking ionosphere reaching receiving station. Reflection and refraction of waves from ionosphere is dependent upon incident angle of transmitted wave, altitude from which it is returned, season, temporal variations due to solar radiations, sunspots and geomagnetic field deviation. In this communication the  $F_2$  layer data recorded at Pakistan Space & Upper Atmosphere Research Commission (SUPARCO) Islamabad Ionosphere Station (SIIS) for the year 2005 has been considered. These data have been used to compute refractive index for hourly observed ordinary wave frequency in the range of (3.04 to 8.29 MHz). The geographic position of SIIS is latitude 33.75 °N and longitude 72.87 °E. To get insight parametric relationship, exploratory data analysis has been performed. The estimation of parametric variability is modeled using standard technique; data distribution, trend, regression and stochastic analysis. This study helps us in predicting and forecasting sky wave propagation for this region.

**Index Terms**— Critical Frequency, Exploratory data analysis, Plasma, Sky wave propagation, Sunspot dynamics, Temporal variations, Total electron count.

## 1 INTRODUCTION

THE existence of ionosphere as electronically conducting region had been postulated earlier in 1883. The ionosphere exists in the altitude of 70 to 600 Km above the sea level. It contains free electrons and ions produced by solar ionizing radiation. Ionosphere regions are designated as C, D, E and F, described by degree of ionization dependent on strength of solar radiations. The most important ionizing agents are ultraviolet,  $\alpha$ ,  $\gamma$  radiation from the sun, cosmic rays and meteors [1]. In the presence of magnetic field, the ionosphere is a doubly refracting medium and two modes of propagation exist; ordinary and extraordinary [2]. The effect of variation in the magnetic field was explained in 1902. The ionosphere tends to be stratified, rather than regular, in its distribution. The layers show electron density peaks, the ionization is the greatest in the summer and day time, least in the winter and night. The sunspot, a standard index of solar activity has direct influence on the radio flux density of ionosphere [3]. In 1924 Appleton, Barnett, Breit and Tuve measured the height of the ionosphere reflecting layers.  $F_2$  region study was carried out during 1972 to 1975 with the help of NASA-AEROS and AEROS B satellites [4]. The ionosphere is a region having refractive index lesser than unity computed with respect of critical frequency of radio wave. In this study for oblique sounding observed critical frequency for the year 2005 over Islamabad region has been used to examine the parameters of interest to present analysis, regression, correlation, modeling and forecasting to obtain results and conclusions.

- Syed Nazeer Alam is an Asstt Prof at Pakistan Navy Engineering College-NUST. Aspiring Phd at ISPA, University of Karachi, Pakistan. e-mail : nazeeralam105@yahoo.com.
- M Ayub Khan Yousufzai, Phd, Space Science, Prof at ISPA, Solar Terrestrial & Atmosphere Wing, University of Karachi, Pakistan. e-mail : ayub-zai@yahoo.com

## 2 THE $F_2$ LAYER

The F layer extends 100 Km to 300 Km and is maintained during day and night. In the daytime, the F region is bifurcated into  $F_1$  and  $F_2$  layers. The  $F_1$  layer is the region extending at altitudes ranging from 150 Km to 210 Km which presents a regular stratification at mid latitudes. The total electron concentration (TEC) in  $F_2$  layer is greater than  $F_1$  layer because of smaller electron loss. In  $F_2$  layer the typical value of electron concentration are  $5 * 10^{11}$  electron/m<sup>3</sup> in the night and  $20 * 10^{11}$  e/m<sup>3</sup> during sun shine and is heavily influenced by a) neutral winds, b) diffusion and c) by different other dynamic affects [4].

## 3 METHODOLOGY

Recorded critical frequency ( $f_o$ ) of  $F_2$  layer using DGS-256 (Transmitter-Receiver equipment) at SIIS has been used to compute electron density ( $N_e$ ) and refractive index ( $\mu$ ) by implementing mathematical relationships. To get insight knowledge of variability of computed parameters, exploratory data analysis has been performed. This analysis has provided complete behaviour of graphical representation of univariate and bivariate modes. The stochastic approach has been utilized to detect the dynamics of data. Smoothing is performed using exponential technique. All these analysis have been performed using Statistica and Minitab software tools.

In our case the peak value of electron density is calculated with respect to measured ordinary wave frequency with the help of expression in Eq-1&2 [1,3 & 5].

$$f_o = \sqrt{80.8N_e} \cong 9 \sqrt{N_e} \quad (1)$$

$$N_e = 1.24 * 10^4 f_o^2 \text{ (MHz)} \text{ e/cm}^3 \quad (2)$$

The computed electron concentration minimum and maximum values are between  $1.1384 \times 10^{11} \text{ e/m}^3$  and  $8.5166 \times 10^{11} \text{ e/m}^3$  with mean of  $3.464 \times 10^{11}$  having standard deviation of  $8.787 \times 10^{10}$ .

### 3.1 Mechanism of Refraction in Ionosphere

The ionosphere consists of weakly and strongly plasma. A vertically launched wave can be reflected and an oblique wave is progressively bent away from the vertical. The amount of refraction depends on three factors, i) the density of ionization of the layer, ii) the frequency of the radio wave, and iii) the angle at which the wave enters the layer. Total refraction occurs when the collision frequency of the ionosphere is less than the radio frequency and if the electron density in the ionosphere is great enough. The velocity of an electromagnetic wave in vacuum is equal to velocity of light ( $c$ ) but in ionosphere medium it is given by  $u = c/\mu$  where ( $\mu$ ) is the refractive index of ionosphere medium rather than property of wave. In the simplified form refractive index mentioned in Eq-3 of ionosphere is given by Appleton-Hartree expression [1, 4 & 5].

$$\mu^2 = 1 - \frac{X(1-X)}{(1-X) - \frac{1}{2} Y_T^2 \pm [\frac{1}{4} Y_T^4 + (1-X)^2 Y_L^2]^{\frac{1}{2}}} \quad (3)$$

The X, Y and Z are magnetoionic parameters defined as:

where,  $X = \frac{N_e e^2}{\epsilon_0 m \omega^2}$

$$Y_L = \frac{e B_L}{m \omega} = Y \cos \phi \quad \text{and} \quad Y_T = \frac{e B_T}{m \omega} = Y \sin \phi$$

Where  $\phi$  is the angle between the propagation direction and the geomagnetic field; then  $\omega_L = \omega_g \cos \phi$  and  $\omega_T = \omega_g \sin \phi$ , in the simplest case, when there are no collisions ( $\nu = 0$ ) and the magnetic field is neglected ( $Y_L = Y_T = 0$ ) the Eq-3 is modified as mentioned in Eq-4 [4&5].

$$\begin{aligned} \mu^2 &= 1 - X = 1 - \omega_N^2 / \omega^2 \\ &= 1 - N_e e^2 / \epsilon_0 m \omega^2 \quad (4) \end{aligned}$$

If the magnetic field is included, the refractive index become double valued. The two waves are called the characteristic waves the upper sign giving the so-called ordinary wave, and the lower sign the extraordinary wave. When collisions are significant ( $\nu \neq 0$ ) the refractive index is complex. The ionosphere is a non magnetic medium the expression (5) explains the dielectric constant ( $k$ ):

$$\mu^2 = c^2 / u^2 = \mu_0 \epsilon / \mu_0 \quad \text{and} \quad \epsilon_0 = \epsilon / \epsilon_0 = k \quad (5)$$

In our case the variation in the computed values of refractive index is 0.9525 to 0.9485 with mean of 0.9501 and a least standard deviation of 0.0005 subject to bending of EM wave in  $F_2$  layer which finally helps in establishing long distance communication. It is observed that signals above the critical angle penetrate the ionosphere layers while below this angle the wave returns to earth. The critical angle for radio wave

depends on electron density of ionosphere layer and wave length of the signal. As the frequency of a radio wave is increased, the critical angle must be reduced for refraction to occur. The maximum useful frequency is related to inclination angle and critical frequency both, expressed in Eq-6.

$$f_{muf} = f_o \text{ Sec } i \quad (6)$$

### 4 EXPLORATORY DATA APPROACH

This approach relies heavily on graphical techniques i.e. plotting of histogram for representation of distribution with single and bivariate quantitative variable. In our study, the sampling distribution of critical frequency and refractive index is witnessed in histogram plots shown in Figs-1&2. The distributions are symmetrical and tend to present Gaussian normal distribution for sample values,  $S=185$ . The variability in ionosphere chemistry due to change in solar radiation, ( $N_e$ ) is subject to change in ( $\mu$ ) has been investigated.

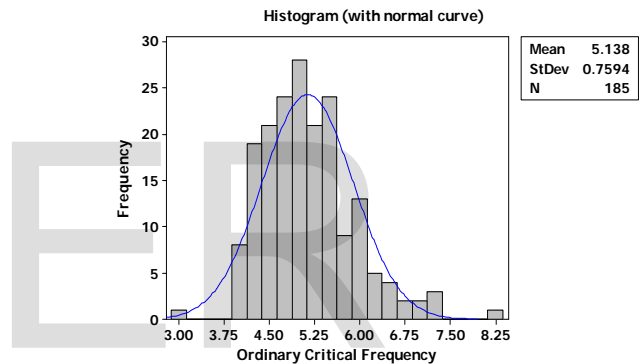


Fig-1: Histogram of observed critical frequency

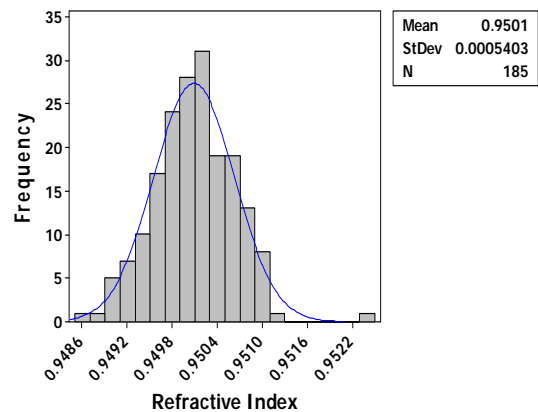


Fig-2: Histogram of computed refractive index

### 4.1 Regression Analysis

The scatter plots are useful diagnostic tool to investigate association between two variables. The computed parameters association with linear fit have been presented in scatter plots of Fig-3&4 [9]. The relationship between refractive index and

critical frequency show a strong negative correlation with  $R^2=95.5\%$  having two outliers, a straight line with intercept of 0.9537 and slope equals to 0.0007, relieve fits through the computed values. This is translated as for decreasing values of refractive index with increaseng critical frequency as shown in Fig-3. The regression line equationnis is given in Eq-7.

$$\mu = 0.9537 - 0.0007f_o \quad (7)$$

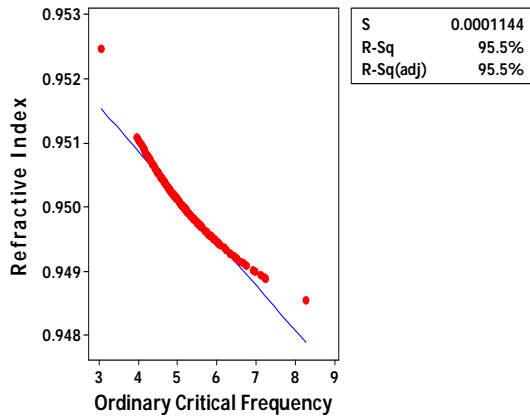


Fig-3: Scatter plot of refractive index and critical frequency

The regression between  $(N_e)$  and  $(\mu)$  is an approximate linear relationship but it reveals a negative correlation statistical condition,  $R^2=89.9\%$  referred to as hetero-scedasticity i.e. non-constant variation in data points [6]. the presence of outliers is due to either measurement error or recording equipment malfunctioning. The regression linear equationnis:

$$N_e = 1.73 * 10^{14} - 1.82 * 10^{15}\mu \quad (8)$$

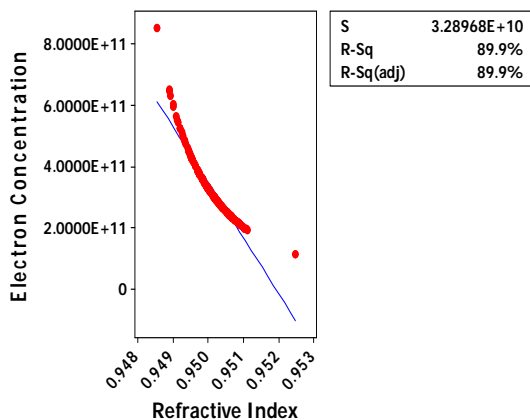


Fig-4: Regression between refractive index and electron concentration

The Pearson’s correlation summary is presented in the Table-1.

Parameters	R <sup>2</sup> (%)	R <sup>2</sup> (adj) %	P
$\mu$ Vs $f_o$	95.8	95.5	0.0000
$N_e$ Vs $\mu$	89.9	89.9	0.0000

## 4.2 Stochastic Aspects

The time domain approach of time series analysis suggests correlation between adjacent points in time is best investigated in terms of a dependence of the current value on the past values. It also focuses on modeling some future value of a time series as parameteric function of the current and previous values [7, 8 &11]. In this communication seasonal pattern with periodic behavior of variation in refractive index against time with linear rising trend and forecast are shown in Fig-5, represents increase and decrease of data in the  $F_2$  layer over Pakistan region.

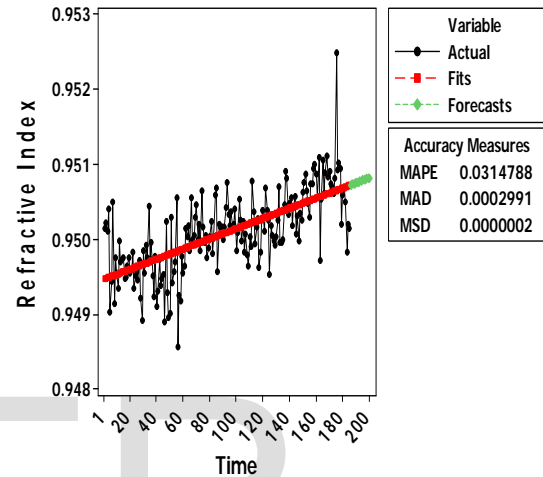


Fig-5: Time series plot of refractive index

## 4.3 Smoothing

It has been observed that non-stationarity presented in time series plots are removed by differencing the data or by fitting some type of trend curve [9]. The time series plots indicate a rising trend for refractive index under investigation. A visual inspection of these plots illustrate that a simple linear fit is sufficient to remove the trend but the variance (amplitude) is still varying with time. The residual plots along with actual time series and smoothed series for fitting with linear trend curve is shown [9].

The smoothing coefficient ( $\alpha$ ) explains degree of smoothing and how responsive the model is to fluctuation in the data sets for computed parameter.

$$F_{t+1} = \alpha Y_t + (1 - \alpha) F_t \quad (9)$$

$$0 < \alpha \leq 1 \quad \text{for } t > 0$$

The smoothing coefficient of refractive index is  $\alpha = 0.18$  for minimum mean percentage error (MPE) and mean absolute percentage error (MAPE) with least residual as shown in Fig-6. The summary of errors is mentioned in Table-2.

Table-2: Summary of errors of refractive index

Summary of Error	Error for $\mu$
MAD	0.00028
MSD	0.0000
MAPE	0.0296

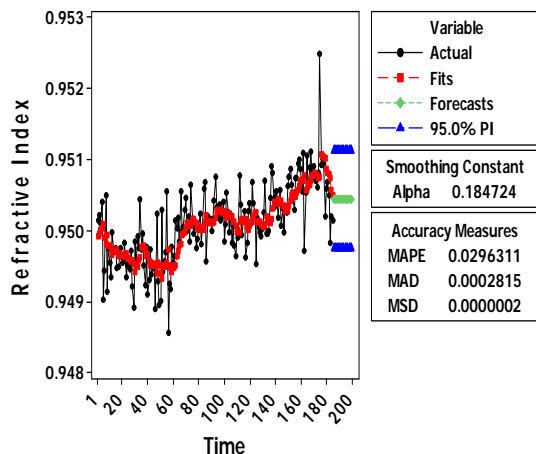


Fig-6: Refractive index - Actual and Exponential Smoothing values

The residual analysis determined by single exponential smoothing shows a sufficiently high degree of correlation and a stable model. The Bootstrapping forecast technique explained in Eq-10 is used to forecast the parameter under study [9].

$$F_{t+1} = F_t + \alpha (X_t - F_t) = F_t + \alpha (e_t) \quad (10)$$

The forecast values with single exponential smoothing for ( $\mu$ ) are computed in Eq-11 using model Eq-10.

$$F_{185} = (0.18) Y_{184} + (0.82) F_{184} \quad (11)$$

$$= 0.950202$$

### 4.3 Model Strategies

There are many methods used to model and forecast time series. The most commonly used model fitting include Box-Jenkins (1976-1996) ARIMA models to handle time-correlated modeling and forecasting. A general ARIMA (p,d,q) model defines autoregression order, difference and moving average respectively. Autoregression process is a stochastic difference equation, a mathematical model in which the current value of a series is linearly related to its past values, plus an additive stochastic shock [9&10].

To estimate, the impact of solar radiation on refractive index of  $F_2$  layer, an autoregressive of order {AR (1)} general model as given in expression (12). A developed stochastic model for ionosphere layer is used to estimate the refractive

index over Islamabad region.

$$X_t = \phi_1 X_{t-1} + \varepsilon_t \quad (12)$$

$\varepsilon_t$ : Source of randomness and is called white noise.

$\phi_1$ : Autoregressive Coefficient

The general model AR (1,0,0) for refractive index, estimates of autoregressive coefficient is 0.99995.

### 4.4 Forecasting

In the time series of Fig-7 follow a repeating pattern,  $X_t$  is highly correlated with  $X_{t-cycle}$ . To create time series model such that the error between the predicted value of the variable and the actual value is as small as possible [8]. The model use lag values of refractive index and used as predictor variable. The refractive index forecast values are represented in Table-3.

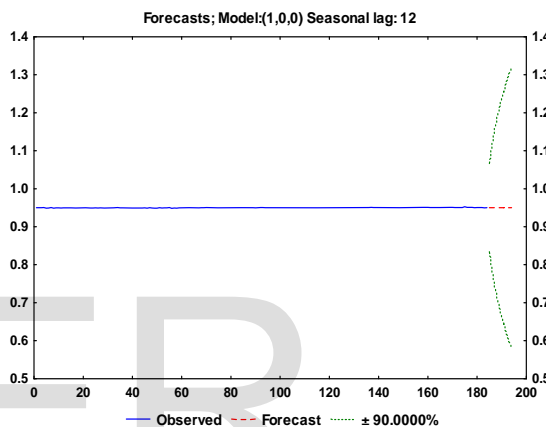


Fig-7: Forecasting graph of refractive index

Table-3: Forecasting values of refractive index

Sample No	Forecast
185	0.950202
186	0.950202
187	0.950201
188	0.950201
189	0.950201
190	0.950201
191	0.950200
192	0.950200
193	0.950200
194	0.950200

An autocorrelation is the correlation between the target variable, refractive index and its lag values. Correlation values range from -1 to +1 show that two variables move together perfectly. In the presentation the estimated correlation between  $i^{th}$  observation and the  $(i + m)^{th}$  observation on the Y-axis vs the lag number on the X-axis [9&10]. On examining autocorrelation illustrated in Fig-8 the highest autocorrelation is + 0.582 which occurs with a lag 1. Hence we desire to be sure to include lag values up to 1 when building the model. The second column of the autocorrelation indicates positive significant autocorrelations occurred for lag 1 to 15. The sta-

tistical significance (Q statistical) is mentioned on the right hand side.

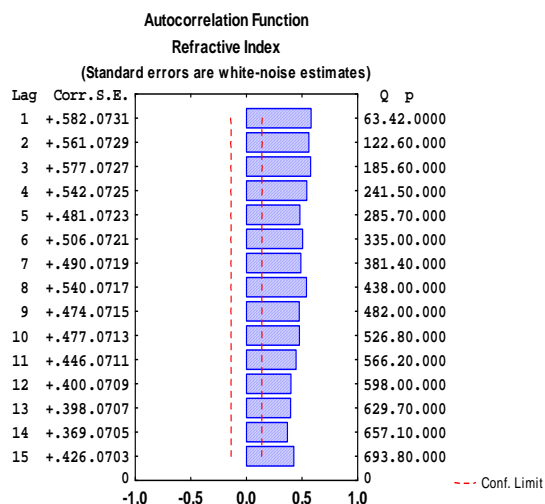


Fig-8: Autocorrelation function of refractive index

The partial autocorrelation is autocorrelation of time series observations separated by a lag of k time units with the effects of the intervening observations disqualified [9]. The partial autocorrelation plot shown in Fig-9 witness statistical significance for 1 to 3 & 8 and all other lags are within 95% confidence interval bands.

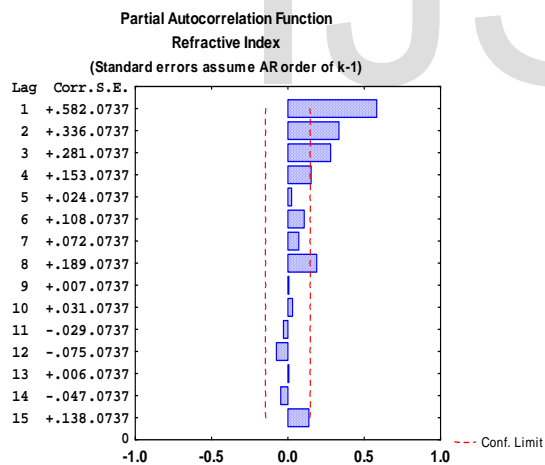


Fig-9: Partial autocorrelation function of refractive index

## 5 RESULTS and CONCLUSION

The presence of ionosphere and change in its characteristics with time has been inspected a potential source for high frequency wave propagation. This communication has revealed physical behavior of ionosphere at Pakistan region. The results determined the values mentioned in the tables and visible from the graphical interpretations.

The exploratory data analysis has been performed and the models have been developed for predicting & forecasting the

ionospheric conditions mentioned above. This has provided a comprehensive behavior of the process. It has been argued that this methodology adapted for providing suitable judgement for the measure values of critical frequency to compute refractive index. The computed values of parameters are found reasonably accurate. It is seen that the ARIMA (1) is found suitable for predicting and forecasting for ionosphere parameter under study.

## ACKNOWLEDGEMENT

The authors are grateful to the officials of Pakistan Space & Upper Atmosphere Research Commission for provision of ionosphere data.

## REFERENCES

- [1] Robert W. Schunk, Andrew F. Naagy, Ionosphere Physics, Plasma Physics and Chemistry, ISBN 0 521 607701, Cambridge University Press, 2004, PP 28-30.
- [2] Henry Rishbeth and Owen K. Garriott, Academic Press Inc, Library of Congress No 69-12280 111 Fifth Avenue New York, 10003, USA, 1969, PP 47-50.
- [3] Les Barclay, Propagation of Radio Waves, 2<sup>nd</sup> Ed, ISBN 0 85296 102 2, Published by the Institution of Electrical Engineers, London, United Kingdom, 2003, PP 312-321.
- [4] M Dolukhanov, Propagation of Radio waves, Translated by Boris Kuznetsov, Mir Publication, Moscow, 1971, PP 213-218.
- [5] H. Sizon, Radio Wave Propagation for Telecommunications Applications, ISBN 3-540-40758-8 Springer Heidelberg New York, USA, 2005, PP 69-75.
- [6] P.N. Arora et al; Comprehensive Statistical Methods, 1st Ed, ISBN 81-219-2776-5, New Delhi, India, 2007, PP 8.1-8.6.
- [7] Allen H Murphy and Richard W. Katz, Probability Statistics and Decision Making in the atmospheric Sciences ISBN: 0-86531-153-6, published by Westview Press, USA, 1985, PP 189-191.
- [8] Francis X. Diebold, Elements of Forecasting, ISBN 0538-86244-0 South-western College Publishing, Cincinnati Ohio, USA, 1998, PP 194-202.
- [9] Spyros Makridakis et al; Forecasting: Methods and Applications, 2<sup>nd</sup> Ed published by John Wiley & Sons, New York, 1983, PP 84-93; 217-219; 413-418.
- [10] R H Shumway and David S. Stoffer, Time Series analysis and its Applications with R Examples, 2<sup>nd</sup> Ed, ISBN 978-818489-025-9 Published by Springer (India) Private Limited, 2008, PP 11-12; 143-151.
- [11] Georg E.P. Box et al; 3<sup>rd</sup> Ed, ISBN 81-317-1633-3, Pearson Education Inc and Dorling Kindersley published, Inc, 2007, PP 21-25.
- [12] S.H.C. du Toit et al; Graphical Exploratory data analysis, ISBN 0-387-96313-8 Springer Verlag New York Berlin Heidelberg, 1986.